

## Synthesis, crystallographic and spectroscopic data, solubility, and electrokinetic properties of metakahlerite and its Mn analogue

RENAUD VOCHTEN

Laboratorium voor Chemische en Fysische Mineralogie, Universiteit Antwerpen,  
Middelheimlaan 1, B-2020 Antwerpen, Belgium

EDDY DE GRAVE

Laboratorium voor Magnetisme, Rijksuniversiteit Gent, Proeftuinstraat 86,  
B-9000 Gent, Belgium

JOZEF PELSMAEKERS

Studiecentrum voor Kernenergie, Boeretang 200, B-2400 Mol, Belgium

### ABSTRACT

Manganese uranyl arsenate,  $\text{Mn}(\text{UO}_2\text{AsO}_4)_2 \cdot 8\text{H}_2\text{O}$ , and metakahlerite,  $\text{Fe}(\text{UO}_2\text{AsO}_4)_2 \cdot 8\text{H}_2\text{O}$ , have been synthesized from reagent-grade chemicals. Fully oxidized metakahlerite is obtained by oxidation with  $\text{H}_2\text{O}_2$ . The three arsenates have been investigated by X-ray powder diffraction, infrared spectroscopy, zeta-potential measurements, and thermal analyses. The  $^{57}\text{Fe}$  Mössbauer spectra at 80 and 300 K have been recorded for the Fe-containing samples.

Metakahlerite and manganese uranyl arsenate have the same tetragonal structure with cell parameters  $a = b = 20.25(1) \text{ \AA}$  and  $c = 17.20(1) \text{ \AA}$ ,  $Z = 16$ ,  $V = 7057(7) \text{ \AA}^3$  and a measured density of  $3.77 \text{ g/cm}^3$ . The fully oxidized phase of metakahlerite has a triclinic symmetry with space group  $c1-P1$  and cell parameters  $a = 7.44(1) \text{ \AA}$ ,  $b = 9.94(1) \text{ \AA}$ ,  $c = 7.37(1) \text{ \AA}$ ,  $\alpha = 94.7(1)^\circ$ ,  $\beta = 102.7(1)^\circ$ ,  $\gamma = 90.3(1)^\circ$ . The measured and calculated densities are  $3.19$  and  $3.18(7) \text{ g/cm}^3$ , respectively. The structural change upon oxidation qualitatively explains the features observed from infrared and Mössbauer spectroscopy.

The solubility products for metakahlerite and manganese uranyl arsenate are  $10^{-44.73}$  and  $10^{-42.43}$ , respectively. For both compounds, the zeta-potential remains negative between  $\text{pH} = 3$  and  $\text{pH} = 9$ . The oxidation of metakahlerite is also clearly reflected in the variation of the zeta-potential.

### INTRODUCTION

Kahlerite,  $\text{Fe}(\text{UO}_2\text{AsO}_4)_2 \cdot 12\text{H}_2\text{O}$ , and its "meta" form with eight molecules of water are members of the meta-autunite group and may be considered as the arsenate analogues of bassetite,  $\text{Fe}(\text{UO}_2\text{PO}_4)_2 \cdot 8\text{H}_2\text{O}$ . As for all uranyl arsenates, metakahlerite is formed as an indirect product from the weathering of relatively rare As- and U-bearing minerals and is therefore an uncommon mineral as well. To the best of our knowledge, it has only been found in the oxidation zone of the siderite deposit of Hüttenberg, Kärnten, Austria (Meixner, 1940, 1953), and the Sophie mine, Wittichen, Germany (Walenta, 1958).

Meixner (1940, 1953) described metakahlerite as a secondary mineral, mostly associated with arseniosiderite ( $\text{Ca}_3\text{Fe}_4(\text{OH})_6(\text{AsO}_4)_4 \cdot 3\text{H}_2\text{O}$ ), scorodite ( $\text{Fe}(\text{AsO}_4) \cdot 2\text{H}_2\text{O}$ ), and other iron arsenates. The arsenate and uranyl ions are believed to originate from the oxidation of löllingite ( $\text{FeAs}_2$ ) and uraninite ( $\text{UO}_2$ ), which are both associated with siderite ( $\text{FeCO}_3$ ). According to the author, metakahlerite crystallizes as tetragonal, nonfluorescent plates with a yellow-brown color.

Referring to a previous study on copper, cobalt, and

nickel uranyl arsenates (Vochten and Goeminne, 1984), the present paper describes a similar study on iron uranyl arsenate and, in addition, on its oxidation mechanism. For the matter of completeness, the manganese member of the uranyl arsenates has been considered as well, although this compound has not been found yet in nature. Sufficient reference material was synthesized either directly from pure chemicals or by ion-exchange reaction on trögerite. The final products were characterized by chemical analysis, X-ray diffraction, infrared and  $^{57}\text{Fe}$  Mössbauer spectroscopy. The solubility constants and the zeta-potentials under different conditions have been determined.

### SYNTHESIS

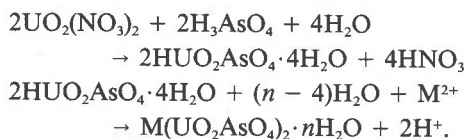
The meta form of both iron and manganese uranyl arsenate was synthesized starting from reagent-grade chemicals or by cation-exchange experiments on trögerite ( $\text{HUO}_2\text{AsO}_4 \cdot 4\text{H}_2\text{O}$ ) at  $100^\circ\text{C}$ . For the direct synthesis, 1 L  $0.10 \text{ M}$   $\text{H}_3\text{AsO}_4$ , neutralized with  $\text{NaOH}$  to  $\text{pH} 5$ , and 1 L  $0.02 \text{ M}$   $\text{UO}_2(\text{NO}_3)_2 \cdot 6\text{H}_2\text{O}$  were added separately but simultaneously to 1 L of a boiling solution of  $0.01 \text{ M}$   $\text{FeSO}_4$  containing 2-g ascorbic acid. The reaction mixture

Table 1. Chemical analyses of synthetic manganese and iron uranylarsenate and fully oxidized iron uranylarsenate

oxide	Mn uranylarsenate			Fe uranylarsenate			Oxidized Fe uranylarsenate		
	wt. %	atomic ratios <sup>1)</sup>		wt. %	atomic ratios <sup>1)</sup>		wt. %	atomic ratios <sup>1)</sup>	
MnO	6.72	Mn	0.942	—	—	—	—	—	—
FeO	—	—	—	7.29	Fe <sup>2+</sup>	0.989	—	—	—
Fe <sub>2</sub> O <sub>3</sub>	—	—	—	—	—	—	8.06	Fe <sup>3+</sup>	0.965
UO <sub>3</sub>	56.47	U	2.079	57.04	U	2.056	56.30	U	1.879
As <sub>2</sub> O <sub>5</sub>	22.29	As	1.928	22.87	As	1.931	22.78	As	2.025
H <sub>2</sub> O	14.28	H <sub>2</sub> O	1.980	14.41	H <sub>2</sub> O	7.786	14.08	H <sub>2</sub> O	6.892
								OH <sup>-</sup>	0.950
Total	100.12			101.61			101.22		
Chemical Formula	16 Mn (UO <sub>2</sub> AsO <sub>4</sub> ) <sub>2</sub> · 8H <sub>2</sub> O			16 Fe (UO <sub>2</sub> AsO <sub>4</sub> ) <sub>2</sub> · 8H <sub>2</sub> O			16 Fe (UO <sub>2</sub> AsO <sub>4</sub> ) <sub>2</sub> (OH) · 7H <sub>2</sub> O		
Density g · cm <sup>-3</sup>	3.76 ± 0.05			3.73 ± 0.05			3.19 ± 0.05		

1) Formula calculated on the basis of 12 oxygen atoms per formula unit  
2) Unit-cell constants, a = b = 20.25, c = 17.20 Å

was then refluxed for 48 h, after which time a crystalline precipitate had formed. After filtration, the precipitate was washed with distilled water and air dried. In order to avoid any oxidation, all manipulations were carried out in a constant N<sub>2</sub> atmosphere. Manganese uranyl arsenate was prepared similarly, using MnSO<sub>4</sub> instead of FeSO<sub>4</sub> under ambient atmosphere. The formation of M(UO<sub>2</sub>AsO<sub>4</sub>)<sub>2</sub> · nH<sub>2</sub>O, with M = Fe<sup>2+</sup> or Mn<sup>2+</sup>, can generally be represented as



Fully oxidized metakahlerite was obtained by treating an aqueous suspension of the nonoxidized phase with 10% H<sub>2</sub>O<sub>2</sub> for 48 h. The oxidation mechanism is suggested to be

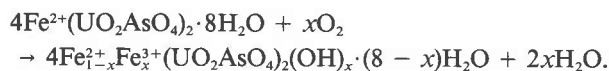


Table 2. DSC and TGA data for synthetic manganese and iron uranyl arsenate and fully oxidized iron uranyl arsenate

	DSC	TGA	Loss of moles H <sub>2</sub> O per formula unit	
	endothemic reaction (°C)	temperature interval (°C)		
Mn(UO <sub>2</sub> AsO <sub>4</sub> ) <sub>2</sub> · 8H <sub>2</sub> O	58	25 - 75	1.20	8.07
	100	75 - 105	3.90	
	210	150 - 330	2.97	
Fe(UO <sub>2</sub> AsO <sub>4</sub> ) <sub>2</sub> · 8H <sub>2</sub> O	50	25 - 75	1.02	8.01
	110	75 - 195	3.97	
	225	195 - 365	3.02	
Fe(UO <sub>2</sub> AsO <sub>4</sub> ) <sub>2</sub> (OH) · 7H <sub>2</sub> O	68	25 - 95	1.06	7.50
	85	95 - 160	1.94	
	170	160 - 190	0.60	
	210	190 - 500	3.90	

On complete oxidation (x = 1), the obtained product has a lemon-yellow color and is nonfluorescent.

### CHEMICAL ANALYSIS

The air-dried species were dissolved in 6 M HCl in which the MnO, FeO, UO<sub>3</sub> and As<sub>2</sub>O<sub>5</sub> contents were determined. The MnO content was evaluated by atomic absorption spectroscopy. The FeO content was determined according to the titrimetric method of Pratt (1894), whereby Fe<sup>3+</sup> is titrated in a boric-phosphoric acid medium by K<sub>2</sub>Cr<sub>2</sub>O<sub>7</sub>, using barium diphenylamine sulfonate as an indicator. The total Fe content is determined by the volumetric method of Hume and Kolthoff (1957) from which the Fe<sub>2</sub>O<sub>3</sub> content is obtained in a straightforward manner. The solution was spectrophotometrically analyzed for UO<sub>3</sub>, using arsenazo III as the reagent. The optical density was measured at 662.5 nm (Jeffrey, 1975). The percentage of As<sub>2</sub>O<sub>5</sub> was determined according to the molybdenum-blue method, the optical density being measured at 840 nm (Jeffrey, 1975). The water content is obtained from thermogravimetric analysis (TGA). Finally, the chemical formula of the synthesized species was calculated from the oxide composition, using the method of Bulach (1964). Table 1 summarizes the results of the chemical analyses, together with the density obtained by subsequent weighing of the specimens in air and toluene using a micro electrobalance (Cahn-RG). It is obvious that the compositions of the synthesized products indeed correspond to the uranyl arsenates aimed for. The relatively low value of the density of the fully oxidized metakahlerite is a first indication that it has a different structure.

### THERMAL BEHAVIOR

Differential scanning calorimetric (DSC) and TGA curves were recorded in a N<sub>2</sub> atmosphere by means of a Du Pont

DSC-910 and TGA-951 apparatus. The rate of heating (5°C/min and 10°C/min) was observed to have no effect on the obtained results, which are listed in Table 2.

As seen, metakahlerite and manganese uranyl arsenate exhibit nearly the same dehydration, characterized by three resolved endothermic peaks. Fully oxidized metakahlerite, however, exhibits an additional endothermic reaction at 170°C (DSC) which can be ascribed to OH<sup>-</sup> leaving the crystal structure. Indeed, within experimental error limits, a release of 0.40 mol of water per formula unit was observed (Table 2), which corresponds to 0.97 mol of OH<sup>-</sup>.

### CRYSTALLOGRAPHIC DATA

Owing to the very small dimensions of the crystals and to the intergrowth of the lamellae, a single-crystal study was not feasible. Therefore, an X-ray powder-diffraction study was performed using a Philips PW-1140 generator with copper radiation ( $K\alpha_1 = 1.5406 \text{ \AA}$ ) in combination with a Ni filter. Si powder (X-ray diffraction standard NBS-640) was used as an internal calibrant. Photographs were obtained with a Guinier-Hägg camera (diameter 100 mm), and the relative intensities of the diffraction lines were measured with a Carl Zeiss Jena MD-100 microdensitometer with resolution  $\Delta\theta \leq 0.050$ .

Both metakahlerite and manganese uranyl arsenate show identical X-ray diffraction patterns, which are moreover identical to the ones obtained for cobalt and nickel uranyl arsenate. This means that these four uranyl arsenates have exactly the same tetragonal structure, so that the different compounds are undistinguishable by X-ray diffraction. Applying the indexing program of Visser (1969) to the subcell parameters  $a_{\text{sub}} = b_{\text{sub}} = 7.16 \text{ \AA}$ , and  $c_{\text{sub}} = 8.60 \text{ \AA}$ ,  $\alpha = \beta = \gamma = 90^\circ$  given by Walenta (1958) for meta-kirchheimerite (JCPDS file no. 12-586), it was impossible to index all reflections. This was observed earlier by Walenta (1964) who suggested that complete indexing is only possible by considering the dimensions of the supercell, i.e.,  $a_{\text{super}} = a_{\text{sub}} \cdot 2\sqrt{2}$  and  $c_{\text{super}} = 2c_{\text{sub}}$ . This is related to the fact that the supercell reflections are very weak and usually difficult to observe. Similar supercell structures are described by Ross (1963) for meta-autunite,  $\text{Ca}(\text{UO}_2\text{PO}_4) \cdot x\text{H}_2\text{O}$ , with  $a_{\text{super}} = b_{\text{super}} = 19.78 \text{ \AA}$  and  $c_{\text{super}} = 16.92 \text{ \AA}$ .

With  $Z = 16$  and  $V = 7057(7) \text{ \AA}^3$ , the density is calculated to be  $3.77 \text{ g/cm}^3$ , which is in good agreement with the observed values (see Table 1). Only copper uranyl arsenate was found to have a distinct X-ray pattern with  $a = b = 7.10(1) \text{ \AA}$  and  $c = 17.42(1) \text{ \AA}$ . According to Ross et al. (1964), the difference in tetragonality is due to the difference in the bonding of copper versus that of Fe<sup>2+</sup> and Mn<sup>2+</sup> and to the resulting effects on the configuration of the interlayer water molecules. Metatorbernite,  $\text{Cu}(\text{UO}_2\text{PO}_4)_2 \cdot 8\text{H}_2\text{O}$ , does not have a supercell ( $a = b = 9.969 \text{ \AA}$ ,  $c = 17.306 \text{ \AA}$ ) nor does meta-zeunerite,  $\text{Cu}(\text{UO}_2\text{AsO}_4)_2 \cdot 8\text{H}_2\text{O}$  ( $a = b = 7.10 \text{ \AA}$ ,  $c = 17.42 \text{ \AA}$ ). These effects might be related to the well-known Jahn-Teller activity of Cu<sup>2+</sup> (Englman, 1972), which favors a  $c/a < 1$  tetragonality.

Table 3. X-ray powder-diffraction data for the phase resulting from fully oxidizing metakahlerite

$I/I_0$	$d_{\text{obs}} (\text{\AA})$	$d_{\text{calc}} (\text{\AA})$	hkl
26	9.770	9.902	010
100	5.925	5.917	$\bar{1}10$
33	5.097	5.100	11 $\bar{1}$
11	4.246	4.244	02 $\bar{1}$
22	3.572	3.569	20 $\bar{1}$
44	3.497	3.498	$\bar{1}2\bar{1}$
100	3.428	3.431	$\bar{2}10$
77	2.960	2.963	102
		2.959	$\bar{2}20$
84	2.535	2.536	03 $\bar{2}$
27	2.464	2.462	30 $\bar{1}$
44	2.369	2.368	01 $\bar{3}$
33	2.322	2.322	$\bar{1}13$
38	2.247	2.247	30 $\bar{2}$
		2.247	14 $\bar{1}$
27	2.132	2.133	103
35	2.023	2.023	$\bar{3}22$
		2.020	$\bar{1}23$
		2.023	240
33	1.808	1.808	14 $\bar{3}$
11	1.789	1.791	004
		1.791	410
		1.789	014
50	1.761	1.763	214
		1.762	41 $\bar{2}$
16	1.574	1.574	430

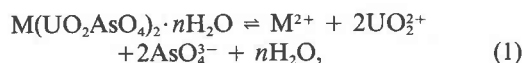
As compared to metakahlerite, the oxidized phase exhibits fewer diffraction lines, some of which are broadened (i.e.,  $d_{\text{hkl}} = 9.902, 3.428, \text{ and } 2.247 \text{ \AA}$ ). The obtained diffraction data are listed in Table 3. From these data, the unit-cell parameters were computed according to the method of McMasters and Larsen (1964), yielding a triclinic symmetry. The space group of the oxidized phase could be either  $P1$  or  $P\bar{1}$ ; the difference cannot be deduced from X-ray powder-diffraction data. The cell parameters were found to be  $a = 7.44(1), b = 9.94(1), \text{ and } c = 7.37(1) \text{ \AA}$  and  $\alpha = 94.7(1)^\circ, \beta = 102.7(1)^\circ, \text{ and } \gamma = 90.3(1)^\circ$ . Using these parameter values in the program of Visser (1969), all 19 observed reflections could be indexed.

The density, calculated for a unit-cell content of  $Z = 1$  and a cell volume of  $530(2) \text{ \AA}^3$ , equals  $3.18(7) \text{ g/cm}^3$ , which agrees well with the value of  $3.19 \text{ g/cm}^3$  measured in toluene.

### SOLUBILITY AND SOLUBILITY CONSTANTS

#### Theoretical consideration

In the pH range 1 to 4, the following equilibrium can be suggested to be responsible for the dissolution of iron and manganese uranyl arsenate.



where M = Fe<sup>2+</sup> or Mn<sup>2+</sup>. The solubility constant  $K_s$  is given by

$$K_s = [\text{M}^{2+}][\text{UO}_2^{2+}]^2[\text{AsO}_4^{3-}]^2. \quad (2)$$

Since the AsO<sub>4</sub><sup>3-</sup> ion is protonated, governed by three

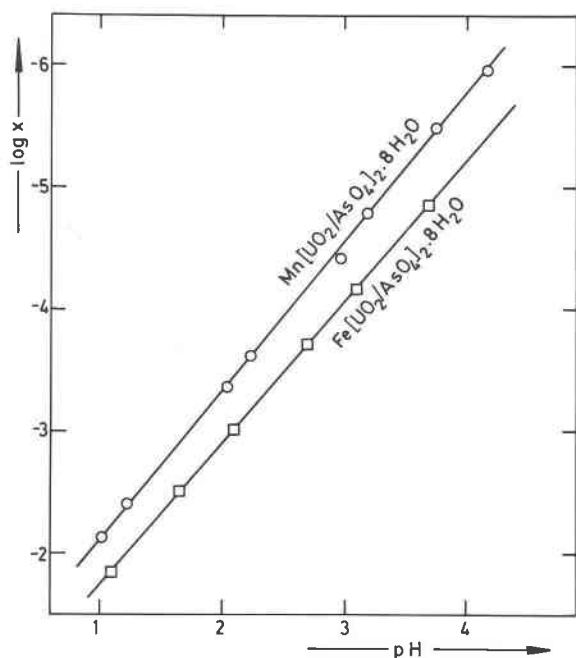


Fig. 1. Variation of the logarithm of the solubility as a function of the pH at 25°C for iron and manganese uranyl arsenate.

equilibria, the solubility of the uranyl arsenates increases markedly with decreasing pH. The relation between the solubility constant  $K_s$ , the solubility  $x$ , the pH, and the stability constants for protonization  $K_i$  is indicated in a previous paper by Vochten and Goeminne (1984) as

$$\log K_s = \log 16 + 5 \log x - 2 \log(1 + K_1^H[H^+]) + K_1^H K_2^H [H^+]^2 + K_1^H K_2^H K_3^H [H^+]^3, \quad (3)$$

where  $K_1^H = 10^{2.19}$ ,  $K_2^H = 10^{6.94}$ , and  $K_3^H = 10^{11.50}$ . The latter equation can be approximated by

$$\log K_s \approx \log 16 + 5 \log x - 2 \log(K_1^H K_2^H K_3^H [H^+]^3) \quad (4)$$

so that

$$\log x \approx -(6/5)pH + \text{constant}. \quad (5)$$

### Experimental details

The solubility of the two uranyl arsenates was determined at 25°C in an initial pH range of 1 to 4. Metakahlerite was equilibrated in a  $N_2$  atmosphere and manganese uranyl arsenate under ambient atmospheric conditions. Periodical measurements of the pH and the composition of the aqueous suspensions revealed that the steady state of the systems was already reached after 2 d. After one week, the suspensions were filtered off, and both the metal ion concentration and the pH were determined. In order to obtain H ion concentrations instead of activities and to eliminate differences in liquid-junction potential in the strong acid medium, the pH values were

Table 4. Solubility and solubility constants at different pH values and at 25°C for iron and manganese uranyl arsenate

pH	5 log x	2 log $[X]^*$	log $K_s$
<b>Fe(UO<sub>2</sub>AsO<sub>4</sub>)<sub>2</sub>·8H<sub>2</sub>O</b>			
1.02	-10.60	35.14	-44.54
1.22	-11.95	33.94	-44.69
1.34	-12.80	33.22	-44.82
2.05	-16.90	28.96	-44.66
2.22	-18.00	22.94	-44.74
2.97	-22.15	23.44	-44.39
3.18	-22.80	22.18	-44.98
3.76	-27.40	18.70	-44.90
4.18	-29.85	16.18	-44.83
<b>Mn(UO<sub>2</sub>AsO<sub>4</sub>)<sub>2</sub>·8H<sub>2</sub>O</b>			
1.19	- 8.00	34.60	-42.60
1.65	-12.55	31.30	-42.65
2.10	-15.00	28.66	-42.46
2.70	-18.40	25.06	-42.26
3.10	-20.90	22.66	-42.36
3.70	-24.20	19.06	-42.26

$$[X]^* = 1 + K_1^H[H^+] + K_1^H K_2^H [H^+]^2 + K_1^H K_2^H K_3^H [H^+]^3$$

measured for a number of different solutions with known acid concentration. A plot of these reference pH values against their actual concentration was used for correcting the experimental values obtained for the uranyl arsenate solutions. The final results are plotted in Figure 1. The observed linearity is consistent with Equation 5, and the slopes, calculated to be  $-1.15$  and  $-1.08$  for iron and manganese uranyl arsenate, respectively, are in good agreement with the theoretical value of  $-1.2$ . The computed solubility constants at different pH values and at 25°C are listed in Table 4. From these, average  $K_s$  values of  $10^{-44.73}$  and  $10^{-42.43}$  are obtained for iron and manganese uranyl arsenate, respectively. Comparing these data with those for copper, cobalt, and nickel uranyl arsenate (Vochten and Goeminne, 1984), i.e.,  $10^{-49.20}$ ,  $10^{-45.34}$ , and  $10^{-45.10}$ , respectively, it is clear that the solubility of iron and manganese uranyl arsenate is approximately the same as for cobalt and nickel uranyl arsenate, whereas the Cu compound exhibits a much lower value.

### ELECTROKINETIC PROPERTIES

In order to obtain information about the surface structure of the mineral particles in suspension, the zeta-potential  $\zeta$  and the surface conductivity  $\lambda_s$  were determined at 25°C under different experimental conditions, according to a method described in a previous paper (Vochten et al., 1984), and the electrophoretic mobilities of the particles in suspension were measured in a thermostated ( $\pm 0.1^\circ\text{C}$ ) cylindrical microelectrophoresis cell (Rank Brothers Mark II).

Since metakahlerite oxidizes very easily, all measurements were carried out in preboiled water in a  $N_2$  at-

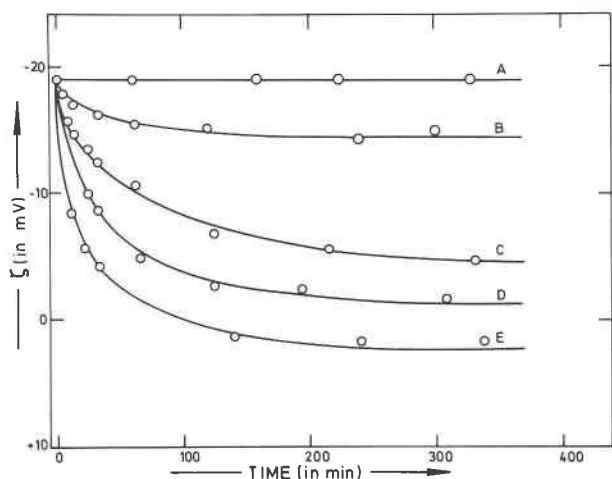


Fig. 2. Variation of the zeta-potential ( $\zeta$ ) as a function of time for metakahlerite under different experimental conditions. (A)  $N_2$  atmosphere, (B) air atmosphere, (C) 0.015%  $H_2O_2$ , (D) 0.030%  $H_2O_2$ , (E) 0.060%  $H_2O_2$ .

mosphere. This procedure prevents any oxidation and results in a time-independent zeta-potential (Fig. 2A). If the experiments are done in water that is in equilibrium with the partial oxygen pressure of the air, the zeta-potential is observed to be time dependent (Fig. 2B).

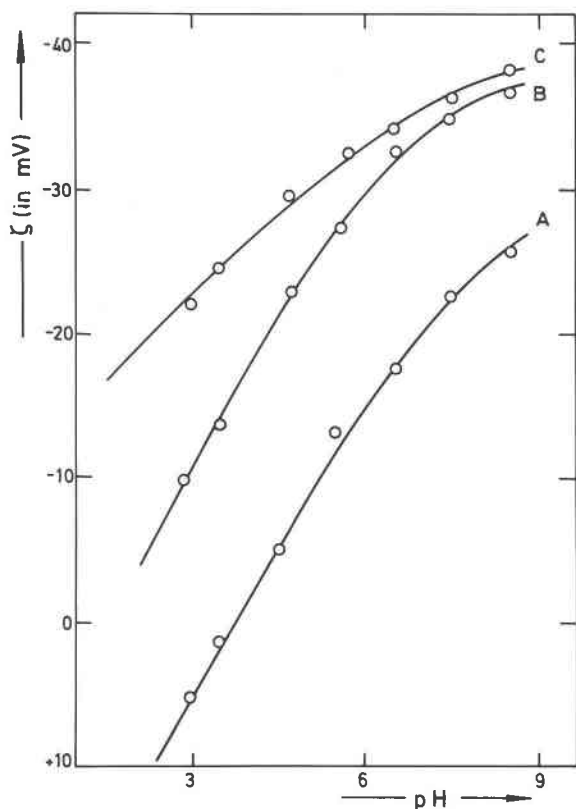


Fig. 3. Variation of the zeta-potential ( $\zeta$ ) at 25°C as a function of the pH for fully oxidized metakahlerite (A), metakahlerite under  $N_2$  atmosphere (B), and manganese uranyl arsenate (C).

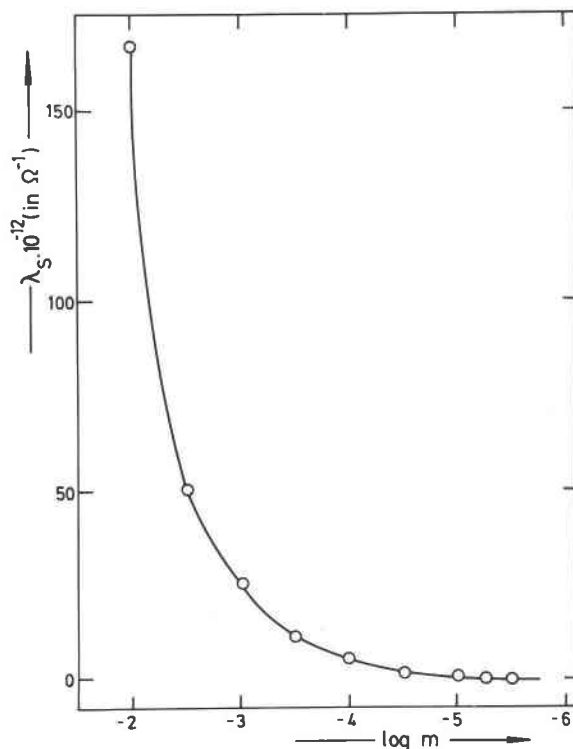


Fig. 4. Variation of the surface conductivity ( $\lambda_s$ ) at 25°C of metakahlerite and its fully oxidized phase as a function of the logarithm of the NaCl concentration.

The oxidation of metakahlerite, being in an aqueous suspension, can be accelerated by the presence of  $H_2O_2$ , which decomposes catalytically into  $H_2O$  and  $O_2$ . This effect is very clearly reflected in Figures 2C, 2D, and 2E, which refer to a  $H_2O_2$  concentration of 0.015, 0.030, and 0.060%, respectively. It is clear that metakahlerite oxidizes very easily in an aqueous medium, even in the absence of oxidants. The oxidation mechanism of the uranyl arsenates in general is discussed in a previous paper by Vochten et al. (1984). As a consequence of the oxidation and the subsequent hydrolysis of  $Fe^{3+}$ , the pH of the suspension decreases significantly. As illustrated in Figure 3, which refers to manganese and iron uranyl arsenate and its fully oxidized phase, the pH indeed has a marked effect on the zeta-potential. The behavior can be explained by a protonization of the negatively charged  $(UO_2AsO_4)_n^{n-}$  layers, thus resulting in a more positive zeta-potential. From the curves in Figure 3, it is seen that for fully oxidized metakahlerite, the point of zero charge is reached only at pH = 3.75, whereas for nonoxidized metakahlerite and manganese uranyl arsenate, this point could not be reached at all.

The surface conductivity  $\lambda_s$  at 25°C and for pH = 4.2, calculated from zeta-potential measurements in NaCl medium, shows no significant differences for synthetic metakahlerite and its fully oxidized phase. As an example, Figure 4 illustrates the variation of the surface conduc-

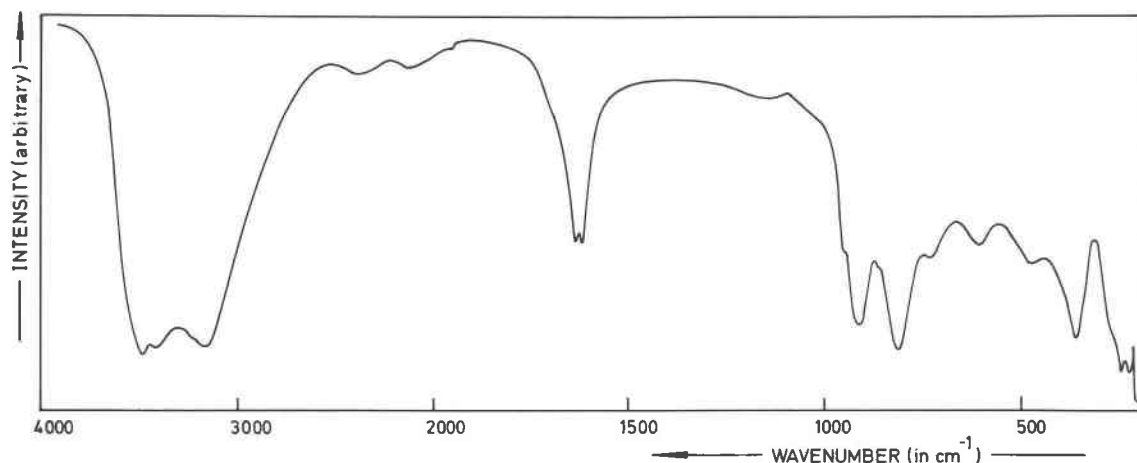


Fig. 5. Infrared spectrum for fully oxidized metakahlerite.

tivity for different NaCl concentrations. The observed equality of the surface conductivity for both compounds leads to the conclusion that the surface structure of metakahlerite does not change markedly with oxidation.

#### INFRARED SPECTROSCOPY

Infrared (IR) spectra in the range 300–4000  $\text{cm}^{-1}$  were recorded with a Perkin Elmer spectrometer. An example is shown in Figure 5 and refers to the sample oxidized from metakahlerite. The IR spectra of iron uranyl phosphate and of copper, cobalt, and nickel uranyl arsenate have been discussed in previous papers (Vochten et al., 1984; Vochten and Goeminne, 1984). Here, it was found that all four compounds exhibit the same IR characteristics in the region 500–3000  $\text{cm}^{-1}$ , except for the absorption bands due to  $\text{AsO}_4^{3-}$  or  $\text{PO}_4^{3-}$ . Some significant differences, however, are observed for oxidized metakahlerite, especially in the broad absorption bands at 3000–3900  $\text{cm}^{-1}$  and at 1640–1680  $\text{cm}^{-1}$ . These regions correspond to the stretching and bending vibrations of water molecules, respectively. For  $\text{Fe}^{2+}(\text{UO}_2\text{AsO}_4)_2 \cdot 8\text{H}_2\text{O}$ , the band maximum is found at 3400  $\text{cm}^{-1}$ , and shoulders appear at 3200 and 3580  $\text{cm}^{-1}$ .

For  $\text{Fe}^{3+}(\text{UO}_2\text{AsO}_4)_2(\text{OH}) \cdot 7\text{H}_2\text{O}$ , two well-resolved overlapping bands are present with maxima at 3140 and

3500  $\text{cm}^{-1}$ . The observed differences are analogous, although less pronounced, to those found earlier for iron uranyl phosphate and its fully oxidized phase (Vochten et al., 1984). A similar explanation can therefore be suggested. As a consequence of the transformation of  $\text{Fe}^{2+}$  into  $\text{Fe}^{3+}$ , the electronic strength of the cations increases, so that a shift of the electronic charge in the OH vibrator toward the cation will take place, thus lowering  $\nu(\text{OH})$  (Maltese and Orville-Thomas, 1967; Lutz et al., 1981). At the same time the stretching vibration of  $\text{OH}^-$  results in an additional band in the region 3500–3600  $\text{cm}^{-1}$  (Lutz et al., 1981). Further, the presence of different kinds of coordination polyhedra can explain the doublet in the bending region (1640–1680  $\text{cm}^{-1}$ ), as already discussed in the case of iron uranyl phosphate.

#### MÖSSBAUER SPECTROSCOPY

##### Experimental details

The  $^{57}\text{Fe}$  Mössbauer spectra for the nonoxidized and for the fully oxidized sample were obtained on a conventional time-mode spectrometer with a triangular reference signal. The source was  $^{57}\text{Co}$  in a Rh matrix. The absorbers had a thickness of 2-mg  $\text{Fe}/\text{cm}^2$ . Spectra were run until an off-resonance count rate of  $\sim 10^6$  per channel (unfolded spectra) was reached. The hyperfine parameters were determined from least-squares fitting of a sum of Lorentzian lines to the experimental data. A modified version of the Wivel and Mørup distribution program (1981) was used to determine the quadrupole distribution for the oxidized phase. All isomer shift values quoted in the text are against  $\alpha\text{Fe}$  at room temperature.

##### Results

The spectra recorded for the nonoxidized and the completely oxidized kahlerite samples, both at 80 K, are shown in Figures 6a and 6b, respectively. At room temperature, the effect observed for the nonoxidized sample is still statistically relevant, although the peak intensity has

Table 5. Isomer shift  $\delta$ , quadrupole splitting  $\Delta E_Q$  and line width  $\Gamma$  for nonoxidized metakahlerite at 80 K and at room temperature ( $\sim 296$  K)

Temperature [K]	$\delta^{(1)}$ [mm/s]	$\Delta E_Q$ [mm/s]	$\Gamma$ [mm/s]
80	1.37 (1) <sup>2)</sup>	2.66 (1)	0.29 (1)
296	1.24 (1)	2.09 (2)	0.28 (1)

1) versus metallic iron at room temperature

2) numbers within ( ) represent the errors on the last digit; they equal 3 times the computed standard deviations.

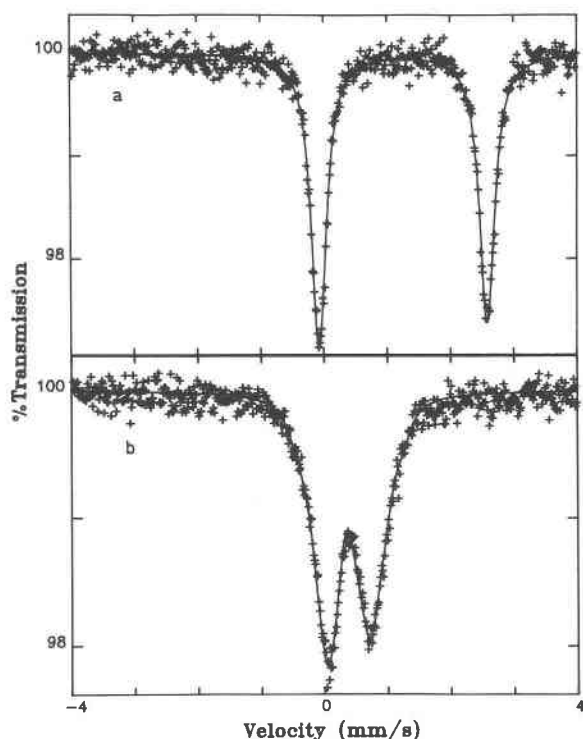


Fig. 6. Mössbauer spectra at 80 K for nonoxidized (a) and fully oxidized metakahlerite (b). Full lines represent the fitted spectra.

dropped to approximately 1% as compared to 2.5% at 80 K. For the second compound, however no reasonable statistics could be obtained, even after extremely long counting times. A combination of three different effects can be held responsible for that behavior: a low Mössbauer fraction  $f$ , the presence of the heavy U and As species, and a wide spread in hyperfine parameters, as will be discussed. For metakahlerite, the latter effect is apparently of no importance as the observed absorption lines are quite narrow. The hyperfine parameters for metakahlerite are listed in Table 5. The 80-K spectrum for the fully oxidized sample could not be fitted in a simple way. The broad and non-Lorentzian line shape results from a distribution in quadrupole splitting values. The significant asymmetry for the line intensities, moreover, indicates that the isomer shift is somehow related to the quadrupole splitting and therefore distributed as well. Attempts to fit a single, discrete distribution of quadrupole doublets, with the isomer shift linearly related to the quadrupole splitting, did not yield a reasonable agreement between calculated and experimental spectral data. A considerable improvement was observed, however, if an additional quadrupole doublet was introduced with a low isomer shift  $\delta = 0.22$  mm/s and a quadrupole splitting  $\Delta E_Q = 1.22$  mm/s. The relative contribution, however, is only 5% so that its Mössbauer parameters are not very accurately determined. The calculated quadrupole distribution profile is plotted in Figure 7, in which the vertical line

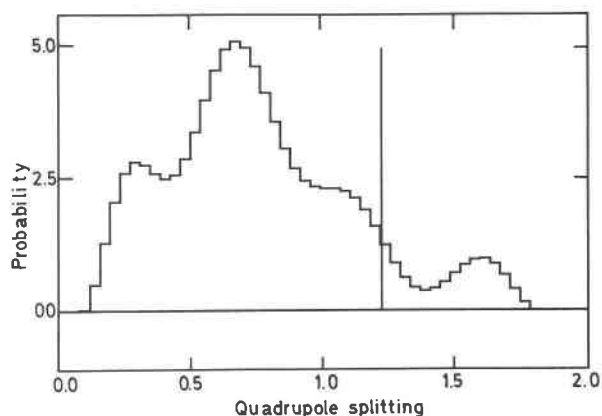


Fig. 7. Quadrupole distribution profile fitted to the 80-K spectrum of the phase obtained from fully oxidizing metakahlerite.

represents the contribution of the additional quadrupole doublet. A total of 45 symmetric doublets with  $\Delta E_Q$  between 0.1 and 1.8 mm/s and with a fixed line width of 0.25 mm/s were considered for the fit. The relation between  $\delta$  and  $\Delta E_Q$ , found to produce a reasonable agreement (full curve in Fig. 6b), was  $\delta = 0.44 + 0.08 \Delta E_Q$ .

Figure 7 shows four maxima at  $\Delta E_Q$  values of 0.41, 0.69, 1.08, and 1.69 mm/s, respectively. However, owing to the rather poor statistics of the spectrum, the significance of this feature may be argued.

## Discussion

Both at 80 K and at room temperature, the nonoxidized kahlerite sample exhibits quite narrow absorption lines, being a synthetic compound, indicating that the chemical and crystallographic environment of  $\text{Fe}^{3+}$  is well defined and very uniform throughout the crystal structure. Both isomer shift and quadrupole splitting are characteristic for an octahedral oxygen coordination. The magnitude of  $\Delta E_Q$  at 80 K points at an orbital singlet ground state for  $\text{Fe}^{2+}$  (Bancroft, 1973). The symmetry being tetragonal, this conclusion further implies that the oxygen octahedron surrounding the  $\text{Fe}^{2+}$  is compressed along the  $c$  axis (Dockum and Reiff, 1979), which is in agreement with the obtained cell parameters.

The Mössbauer spectrum of the oxidized phase displays different structural properties. The broad quadrupole distribution indicates that the  $\text{Fe}^{3+}$  coordination is far from uniform. This is consistent with the line broadening in the X-ray diffraction pattern. Owing to the observed linear relationship between  $\delta$  and  $\Delta E_Q$ , the coordination number is probably the same (at least for 95% of all  $\text{Fe}^{3+}$  species), six being the most likely on the basis of the obtained hyperfine parameters. The observed distribution of the quadrupole splitting must therefore be attributed to a wide range of distortions, probably both in type and magnitude, for the oxygen octahedra surrounding the central  $\text{Fe}^{3+}$  ions. The isomer shift for the additional, nondistributed quadrupole doublet is significantly lower, meaning that a small amount of the Fe could be tetrahedrally coordinat-

ed. This suggestion is rather speculative, but another explanation for the doublet cannot be given at the moment. Finally, it is worthwhile mentioning that the Mössbauer parameters for the kahlerite phases markedly differ from those recently obtained for the corresponding iron uranyl phosphates (Vochten et al., 1984). This is most probably due to the different crystallographic systems involved.

### CONCLUSIONS

The crystallographic, chemical, and IR spectroscopic data of the uranyl arsenates studied in the present and in previous papers are all very similar. An exception to this, however, is the Cu-containing compound. According to the  $^{57}\text{Fe}$  Mössbauer results obtained for metakahlerite, the  $\text{M}^{2+}$  cations are located in an octahedral oxygen coordination that is compressed along the *c* axis. This local symmetry of the  $\text{M}^{2+}$  ions is well defined and very uniform. Metakahlerite is easily oxidized in an aqueous medium that is in equilibrium with the partial pressure of oxygen. The resulting compound displays significantly different chemical and structural properties. The local symmetry around the  $\text{Fe}^{3+}$  species is probably octahedral, however, with a wide range of distortions both in type and magnitude. Despite these marked changes, the surface structure is observed to be rather insensitive to the oxidation.

### ACKNOWLEDGMENTS

Financial support by the National Fund for Scientific Research (Belgium), awarded to R.V. is appreciated. The authors are also indebted to Dr. H. Lauwers for interpretation and discussion of the infrared spectra and to K. Van Springel and C. Van de Veire for technical assistance.

### REFERENCES

- Bancroft, G.M. (1973) Mössbauer spectroscopy. An introduction for inorganic chemists and geochemists, 110–154. McGraw-Hill, London.
- Bulach, A.G. (1964) Berechnung von Mineralformel, 47–50. VEB Deutscher Verlag für Grundstoffindustrie, Leipzig.
- Dockum, B.W., and Reiff, W.M. (1979) A high field Mössbauer study of a six coordinate iron II dithiocarbamate complex and comparison of the  $\text{Fe(II)}\text{S}_6$ ,  $\text{Fe(III)}\text{S}_6$  and  $\text{Fe(IV)}\text{S}_6$  chromophores in tris (diethyl-dithiocarbamate) complexation. *Chemical Physics Letter*, 63, 32–36.
- Englman, R. (1972) The Jahn-Teller effect in molecules and crystals, 1–350. Wiley-Interscience, London.
- Hume, D.N., and Kolthoff, I.M. (1957) The use of cacotheline as an oxidation-reduction indicator before the volumetric oxidation of iron. *Analytica Chimica Acta*, 16, 415–418.
- Jeffrey, P.G. (1975) *Chemical methods of rock analysis*, 481–482. Pergamon Press, Oxford.
- Lutz, H.D., Eckers, W., Schneider, G., and Haeuseller, H. (1981) Raman and infrared spectrum of barium and strontium hydroxides and hydroxide hydrates. *Spectrochimica Acta*, 37A, 561–567.
- Maltese, M., and Orville-Thomas, W.J. (1967) The infrared spectra and structure of some complex hydroxosalts. *Journal of Inorganic and Nuclear Chemistry*, 29, 2533–2544.
- McMasters, O.D., and Larsen, W.L. (1964) Determination of the crystallographic lattice type and cell constants from X-ray powder pattern data, a computer program. U.S. Atomic Energy Commission Report IS-839.
- Meixner, H. (1940) Fluoreszenzanalytische, optische und chemische Beobachtungen an Uranmineralen. *Chemie der Erde*, 12, 433–450.
- (1953) Kahlerit, ein neues Mineral der Uranglimmergruppe, aus der Hüttenberger Erzlagerstätte. *Der Karinthin*, 23, 277–280.
- Pratt, J.H. (1894) On the determination of ferrous iron in silicates. *American Journal of Science*, 48, 284, 149–151.
- Ross, M. (1963) The crystallography of meta-autunite (I). *American Mineralogist*, 43, 1389–1393.
- Ross, M., Evens, H.T., Jr., and Appleman, D.E. (1964) Studies of the torbernite minerals (II): The crystal structure of metatorbernite. *American Mineralogist*, 49, 1603–1621.
- Visser, J.W. (1969) Fully automatic program for finding the unit cell from powder data. *Journal of Applied Crystallography*, 2, 89–95.
- Vochten, R., and De Grave, E. (1981) Crystallographic, Mössbauer and electrokinetic study of synthetic lipscombite. *Physics and Chemistry of Minerals*, 7, 197–203.
- Vochten, R., and Goeminne, A. (1984) Synthesis crystallographic data, solubility and electrokinetic properties of meta-zeunerite, meta-kirchheimerite and nickel uranyl arsenate. *Physics and Chemistry of Minerals*, 11, 95–100.
- Vochten, R., De Grave, E., and Pelsmaekers, J. (1984) Mineralogical study of bassetite in relation to its oxidation. *American Mineralogist*, 69, 967–978.
- Walenta, K. (1958) Die sekundären Uranmineralen des Schwarzwalds. *Jahrbuch der geologisches Landesamt Baden-Württemberg*, 3, 17–51.
- (1964) Beiträge zur Kenntnis seltener Arsenatmineralien unter besonderer Berücksichtigung von Vorkommen des Schwarzwaldes, 1. Folge. *Tschermaks Mineralogische und Petrographische Mitteilungen*, 9(1–2), 111–174.
- Wivel, C., and Mørup, S. (1981) Improved computational procedure for evaluation of overlapping hyperfine parameter distribution in Mössbauer spectra. *Journal of Physics E.: Scientific Instruments*, 14, 605–610.

MANUSCRIPT RECEIVED JUNE 26, 1985

MANUSCRIPT ACCEPTED MARCH 18, 1986